Resonant Characteristics of Circular HTC Superconducting Printed Antenna Covered with a Dielectric Layer

Fadila Benmeddour[1, *], Christophe Dumond[2], and Elhadi Kenane[1]

Abstract—Effects of a superstrate layer on the resonant frequency and bandwidth of a high Tc superconducting (HTS) circular printed patch are investigated in this paper. For that, a rigorous full-wave spectral analysis of superconducting patch in multilayer configuration is described. In such an approach, the spectral dyadic Green's function which relates the tangential electric field and currents at various conductor planes should be determined. Integral equations are solved by a Galerkin's moment method procedure, and the complex resonance frequencies are studied with basis functions involving Chebyshev polynomials in conjunction with the complex resistive boundary condition. To include the superconductivity of the disc, its complex surface impedance is determined by using London's equation and the model of Gorter and Casimir. Numerical results are compared with experimental results of literature as well as with the most recent published calculations using different methods. A very good agreement is obtained. Finally, superstrate loading effects are presented and discussed showing interesting enhancement on the resonant characteristics of the superconducting antenna using combinations of Chebyshev polynomials as set of basis functions.

1. INTRODUCTION

Over the last three decades printed antennas have become an important subject of interest and have been widely used in microwaves and millimeter-waves applications because of their low profile, small size, low weight and low cost [1–4]. However, they suffer from narrow bandwidth, low gain and poor efficiency.

To improve these characteristics, high temperature superconducting (HTS) thin films have been proposed to replace conventional perfectly conducting patch [5–9].

Partly due to their very low surface impedance, smaller losses, smaller dispersion and smaller propagation time have been reported showing that HTS patches are good candidates for current rapid communications. Furthermore, greater performances have been obtained using anisotropic dielectrics or substrate/superstrate configurations for HTS rectangular [10–12] and circular patch [13–15].

For studying the resonant characteristics of antennas in multilayered configuration, different methods have been proposed which can be classified in approximate or full wave approach. Popular approximate models are the transmission-line, the cavity and the segmentation model while the finite element, the finite difference time domain and the moment methods are full-wave ones.

The cavity model and other simple methods provide a simple intuitive understanding of the performance of microstrip antennas. Although the accuracy of these approximate models is limited, they are nevertheless useful in providing the preliminary design and predicting the trends of these characteristics with the variation of design parameters. In contrast, the spectral-domain model is able to analyze arbitrarily shaped geometries and uses the exact Green function for the mixed dielectric

nature of the microstrip antenna. It has been applied extensively and now becomes now a standard approach for the analysis of microstrip geometry especially high-temperature superconducting printed antenna [16, 17]. This method gives better results than approximate techniques.

The rigorous approach developed here is based on the moment method and has already been employed for the study of an HTS circular printed antenna with anisotropic dielectrics [14]. The problem is formulated in terms of integral equations using the vector Hankel transform formalism. A Galerkin's procedure is applied, and the complex resonance frequencies are studied with basis functions in conjunction with the complex resistive boundary condition. The set of basis functions used in this work to expand the disk currents consist of combinations of Chebyshev polynomials with weighting factors to incorporate the edge conditions [14, 18, 19]. These functions as well as the spectral dyadic Green function are efficiently implanted with compact structured Fortran 90. The superconductivity of the patch is taken into account considering a complex surface impedance which is determined by using London's equation and the two-fluid model of Gorter and Casimir [10–15, 20, 21].

The paper is organized as follows: Section 2 presents the mathematical formulation of the problem. In Section 3 numerical results are compared with experimental results [21] seen in literature as well as with the most recent published calculations on this topic using different methods: (1) a CAD model analysis [15] and (2) a similar full wave analysis but using a different type of expansion basis functions [20]. Finally, in Section 4 the effects of a protective dielectric superstrate on the resonance frequency and bandwidth of a HTS circular printed antenna are presented and discussed and conclusions are given in Section 5.

2. THEORY

The geometry under consideration is illustrated in Figure 1. A circular superconducting patch of thickness e is printed on a grounded dielectric slab of thickness h_1. The substrate is characterized by the free-space permeability μ_0 and a permittivity $\varepsilon_0 \varepsilon_{r1}$. Above the radiating patch is the superstrate layer of thickness h_2 with permeability μ_0 and a permittivity $\varepsilon_0 \varepsilon_{r2}$ and a normal state conductivity σ_n. The superconducting film is characterized by a critical temperature Tc, a zero-temperature penetration depth λ_0.
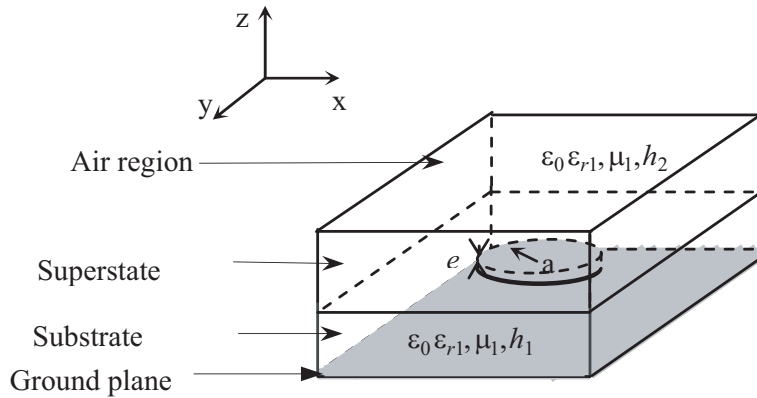
Figure 1. Geometrical structure of HTS superstrate loaded circular printed antenna on a uniaxial substrate.

The permittivity tensor in this region is given by:

$$\bar{\varepsilon} = \varepsilon_0 \text{diag}\left[\varepsilon_x, \varepsilon_x, \varepsilon_z\right] \tag{1}$$

A relation between the surface electric field at the plane of the HTS patch and the surface current on the patch in the spectral domain is given by [12]:

$$e_n(\rho) = \int_0^\infty dk_\rho k_\rho \bar{H}_n(k_\rho \rho) \cdot \left(\bar{G}(k_\rho) - \bar{Z}_s\right) \cdot \mathbf{K_n}(k_\rho) = 0 \quad \rho < a \tag{2}$$

$$\kappa_n(\rho) = \int_0^\infty dk_\rho k_\rho \bar{H}_n(k_\rho\rho) \cdot \mathbf{K_n}(k_\rho) = 0 \quad \rho > a \tag{3}$$

a: the radius of HTS circular printed antenna;
k_ρ: the spectral variable;
ρ: the spatial variable;
$\bar{H}_n(k_\rho\rho)$: the kernel of the vector Hankel transform;
$\kappa_\mathbf{n}$: the unknown patch currents on the circular disk;
Z_s: the complex surface impedance.
where

$$\bar{Z}_s = \left| \begin{array}{cc} Z_s & 0 \\ 0 & Z_s \end{array} \right| \tag{4}$$

The electric field integral equation which enforces the boundary condition must vanish on the patch surface, as discretized into a matrix form shown as:

$$\left[\begin{array}{cc} \left(\bar{Z}'^{\Psi\Psi}\right)_{M\times M} & \left(\bar{Z}'^{\Psi\varphi}\right)_{M\times P} \\ \left(\bar{Z}'^{\varphi M}\right)_{P\times M} & \left(\bar{Z}'^{\varphi\varphi}\right)_{P\times P} \end{array} \right] \left[\begin{array}{c} (A')_{M\times 1} \\ (B')_{P\times 1} \end{array} \right] = 0 \tag{5}$$

Each element of the submatrices $\bar{Z}'^{CD}_{ij}$ is given by:

$$\bar{Z}'^{CD}_{ij} = \int_0^\infty dk_\rho k_\rho \mathbf{C}^+_{ni}(k_\rho) \cdot \left(\mathbf{G}(k_\rho) - \bar{Z}_s\right) \mathbf{D}_{nj}(k_\rho) \tag{6}$$

where $\mathbf{C}$ and $\mathbf{D}$ represent either $\tilde{\Phi}$ or $\tilde{\Psi}$ for every value of the integer n (Equations (11) and (12)).

The system of linear equation has nontrivial solutions when the determinant of system Equation (5) vanishes, that is:

$$\det\left(\left[\bar{Z}'(f)\right]\right) = 0 \tag{7}$$

In general, the roots of this equation are complex numbers indicating that the structure has complex resonant frequencies.

$$f = f_r + if_i \tag{8}$$

with:

f_r: The resonant frequencies.
f_i: The imaginary parts of the complex resonant frequencies account for damping due to radiation loss.

The half-power bandwidth of a structure operating around its resonant frequency can be approximately related to its resonant frequency through the well-known formula:

$$BW = 2f_i/f_r \tag{9}$$

Applying Galerkin method to solve the vector dual integral Equations (2) and (3), we express the unknown patch currents on the circular disk which are expanding into a finite series of known basis functions as follows [18]

$$\kappa_\mathbf{n}(\rho) = \begin{cases} \displaystyle\sum_{P=1}^{P} a_{np}\Psi_{np}(\rho) + \sum_{q=1}^{q} b_{nq}\Phi_{nq}(\rho) & a < \rho \\ 0 & \rho > a \end{cases} \tag{10}$$

a_{np} and b_{nq} are the mode expansion coefficients.

The basis functions consist of combinations of Chebyshev polynomials, with weighting factors to incorporate the edge condition. It has been shown that these functions give convergent results using a moderate number of terms in the current expansion [14, 18, 19].

With:

$$\Psi_{np}(\rho) = \begin{cases} \begin{bmatrix} (\rho/a)^{n-1} U_{2p-1}(\rho/a) \sqrt{1-(\rho/a)^2} \\ 0 \end{bmatrix} & \rho < a \quad n \in \mathbf{N}^*, \quad p = 1,2,3,\ldots,P \\ 0 & \rho > a \end{cases} \tag{11}$$

$$\Phi_{nq}(\rho) = \begin{cases} \begin{bmatrix} 0 \\ i\,(\rho/a)^{n-1} \dfrac{T_{2q-2}(\rho/a)}{\sqrt{1-(\rho/a)^2}} \end{bmatrix} & \rho < a \quad n \in \mathbf{N}^*, \quad q = 1,2,3,\ldots,Q \\ 0 & \rho > a \end{cases} \tag{12}$$

where $\mathbf{T}$ and $\mathbf{U}$ in Equations (11) and (12) are respectively the Chebyshev polynomials of the first and second kinds.

Consider the evaluation of the VHT of Equations (11) and (12). The basis functions given in Equations (13) and (14) are then Hankel transformed to obtain $\tilde{\Psi}_{np}$ and $\tilde{\Phi}_{nq}$, whose expressions are given by [14].

$$\tilde{\Psi}_{np}(k_\rho) = \frac{a^2}{2} \begin{bmatrix} \int\limits_0^1 dx\,x^{n-1} U_{2p-1}(x) \sqrt{1-x^2} J_{n-1}(\xi x) - \int\limits_0^1 dx\,x^{n-1} U_{2p-1}(x) \sqrt{1-x^2} J_{n+1}(\xi x) \\ i\left[\int\limits_0^1 dx\,x^{n-1} U_{2p-1}(x) \sqrt{1-x^2} J_{n-1}(\xi x) + \int\limits_0^1 dx\,x^{n-1} U_{2p-1}(x) \sqrt{1-x^2} J_{n+1}(\xi x)\right] \end{bmatrix}$$

$$n \in \mathbf{N}^*, \quad p = 1,2,3,\ldots,P \tag{13}$$

$$\tilde{\Phi}_{nq}(k_\rho) = \frac{a^2}{2} \begin{bmatrix} -i\left[\int\limits_0^1 dx\,x^n \dfrac{T_{2q-2}(x)}{\sqrt{1-x^2}} J_{n-1}(\xi x) + \int\limits_0^1 dx\,x^n \dfrac{T_{2q-2}(x)}{\sqrt{1-x^2}} J_{n+1}(\xi x)\right] \\ \int\limits_0^1 dx\,x^n \dfrac{T_{2q-2}(x)}{\sqrt{1-x^2}} J_{n-1}(\xi x) - \int\limits_0^1 dx\,x^n \dfrac{T_{2q-2}(x)}{\sqrt{1-x^2}} J_{n+1}(\xi x) \end{bmatrix}$$

$$n \in \mathbf{N}^*, \quad q = 1,2,3,\ldots,Q \tag{14}$$

with: $\xi = k_\rho a$.

To include the effect of the superconductivity of the patch in full-wave analysis, complex surface impedance is defined as the ratio of $|\mathbf{E}|$ to $|\mathbf{H}|$ for the case of an incident plane wave normal to the surface. It is given by:

$$Z_s = R_s + X_s \tag{15}$$

with R_s and X_s which are respectively the surface resistance and the surface reactance.

Moreover when the thickness t of the superconducting patch is less than three times the penetration depth λ_0 at a temperature $T = 0\,\mathrm{K}$, the surface impedance can be approximated as follows:

$$Z_s = \frac{1}{t\sigma} \tag{16}$$

while conductivity σ is a real number for conventional conductors, which has been verified for practical metallization thicknesses by comparison with rigorous mode matching result. The complex conductivity σ of the superconducting film is determined by using London's equation and the model of Gorter and Casimir as [21]:

$$\sigma = \sigma_1 - i\sigma_2 \tag{17}$$

σ_1 may arise from normal electron conduction within non-superconducting grains and scattering from grain boundaries, flux vibration at pinning centers and normal electron conduction due to thermal agitation in the superconducting state. The reactive part of the conductivity $(-i\sigma_2)$ arises from the

lossless motion of the superconducting carries which may be derived from the Lorentz-force equation as [14, 20, 21]:

$$\sigma_1 = \sigma_n \left(T/T_c\right)^4 \tag{18}$$

and

$$\sigma_2 = \frac{1 - \left(T/T_c\right)^4}{\omega \mu_0 \lambda_0^2} \tag{19}$$

where

σ_n: is often associated with the normal state conductivity at the transition temperature of the superconductor T_c.

ω: is the angular frequency.

3. RESULTS AND DISCUSSION

To validate our numerical approach for a perfectly conductive printed antenna covered by a dielectric protective layer, measurements were carried out at the PRISME institute of University of Orleans. Perfect conducting circular printed antennas with radius $a = 50\,\text{mm}$ were printed with classic circuit process, alimented by coax-fed and covered by dielectrics layers of different thicknesses h_2. Same Duroid material with $\varepsilon_r = 2.32$ and thickness $h_1 = 1.57\,\text{mm}$ was used for a substrate and a superstrate. The measured resonant frequencies using an Agilent E5071B vector network are compared with computed ones in Table 1, and a good agreement is obtained, and less than or equal to 2% difference between our measurements results.

In order to confirm the correctness of our results in the case of HTS thin film, Figure 2 presents a comparison with the measurements by Richard et al. [21].

The studied circular patch with a thickness $e = 330\,\text{nm}$ and radius $a = 610\,\mu\text{m}$ is printed on a lanthanum aluminate (LaAlO$_3$) substrate with relative permittivity $\varepsilon_r = 23.81$ and thickness $h_1 = 254\,\mu\text{m}$. A YBCO (YBa$_2$Cu$_3$O$_7$) superconducting thin film with a transition temperature $Tc = 84.5\,\text{K}$, a zero temperature penetration depth $\lambda_0 = 140\,\text{nm}$, and a normal state conductivity $\sigma_n = 10^6\,\text{S/m}$ is considered.
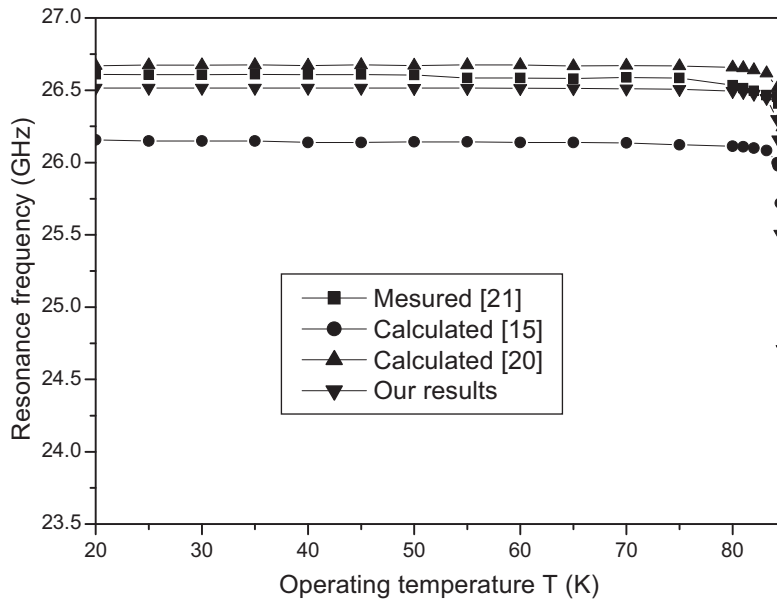
Figure 2. Resonant frequency for a circular printed superconducting patch antenna as a function of the operating temperature; $\varepsilon_r = 23.81$, $h_1 = 254\,\mu\text{m}$, $a = 610\,\mu\text{m}$, $e = 330\,\text{nm}$, $\lambda_0 = 140\,\text{nm}$, $T_c = 84.5\,\text{K}$, $\sigma = 10^6\,\text{S/m}$.

Furthermore, in Figure 2, our results are also confronted with those of two recent publications on this topic based on: (1) a cavity model approach in [15] and (2) a moment method using the TM and TE modes of cavity as expansion of the disk current [20]. The very good agreement found shows the usefulness of our numerical approach in the study of HTS printed antenna.

The agreement between our results and those measured [21] can be quantified by the average of the resonant frequency relative error, less than 0.6%.

The resonant frequency relative error: $Error(\%) = \left(\frac{\Delta f_r}{f_r}\right) * 100$.
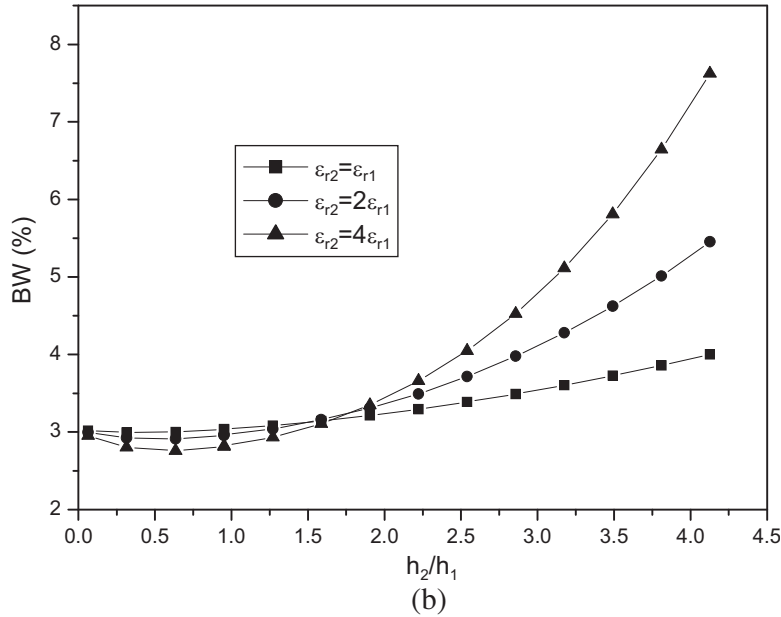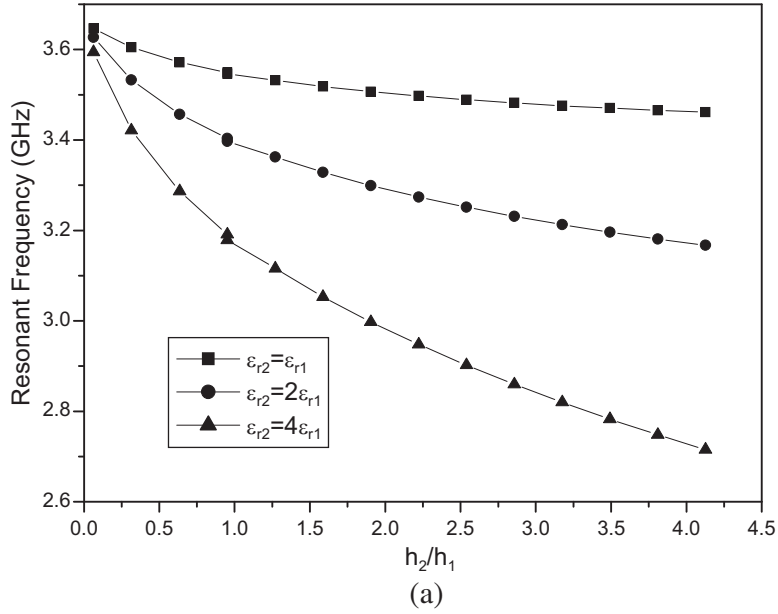
Figure 3. Resonance frequency and half-power bandwidth of the high T_c superconducting printed patch with different thicknesses of superstrate layer against permittivity of superstrate layer; $\sigma_n = 210.10^3$ S/m, $\lambda_0 = 150$ nm, $a = 15$ mm, $\varepsilon_{r1} = 2.32$, $h_1 = 1.5748$ mm, $e = 0.2$ µm. (a) Resonance frequency. (b) Half-power bandwidth.

4. EFFECTS OF A PROTECTIVE DIELECTRIC SUPERSTRATE

In the proposed study, we consider an HTS disc of radius $a = 15$ mm printed on a substrate with thickness $h_1 = 1.5748$ mm and relative permittivity $\varepsilon_{r1} = 2.32$. The superconducting material consists of a thin film of thickness $e = 0.2 \,\mu$m of YBCO characterized by a critical temperature $T_c = 89$ K, an operating temperature $T = 44.5$ K, a zero-temperature penetration depth $\lambda_0 = 150$ nm, and a normal state conductivity $\sigma_n = 210.10^3$ S/m.

Fast numerical convergences are obtained using combinations of Chebyshev polynomials as a set of basis functions with weighting factors to incorporate the edge conditions. Only results for the TM_{11} fundamental resonant mode of the circular patch are presented.

(a)

(b)
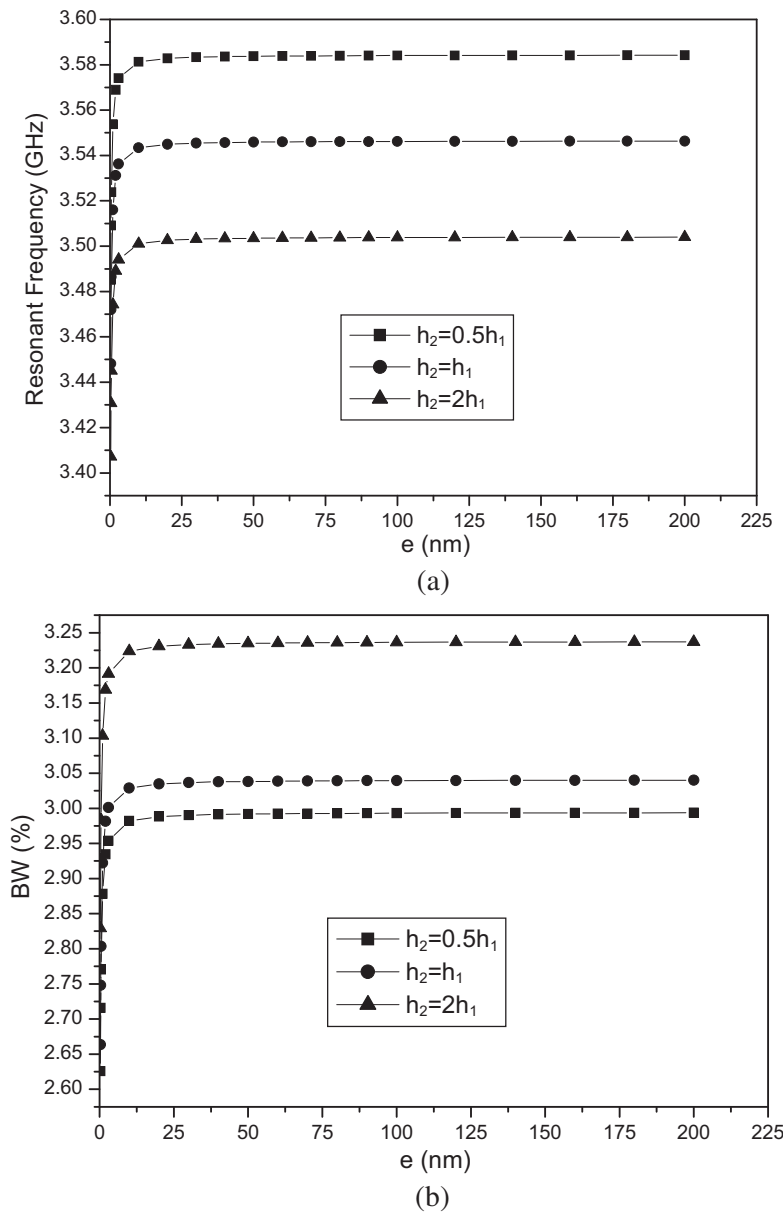
Figure 4. Resonance frequency and half-power bandwidth of the high T_c superconducting microstrip circular patch versus thicknesses of superstrate layer against the thickness of patch. $\sigma_n = 210.10^3$ S/m, $\lambda_0 = 150$ nm, $T/T_c = 0.5$, $a = 15$ mm, $\varepsilon_{1x} = \varepsilon_{1z} = \varepsilon_{2x} = \varepsilon_{2z} = 2.32$, $h_1 = 1.5748$ mm. (a) Resonance frequency. (b) Half-power bandwidth.

Figure 3 depicts the resonant characteristics of superconducting disc for different thicknesses h_2 and permittivity ε_{r2} of superstrate.

Results show that in addition to its protective action, the presence of a dielectric cover has two major interests in the field of antennas: (1) it decreases the resonant frequency which allows a reduction in the patch size for the same target frequency, and (2) it increases the half-power bandwidth which improves the narrow-band characteristics of printed antenna. It can be observed in both Figures 3(a) and 3(b) that these effects are more pronounced for thicker superstrate and for increasing ratio of $\varepsilon_{r2}/\varepsilon_{r1}$. As it is well-known in printed antenna design, a low value of substrate permittivity ε_{r1} is generally preferred because it increases the fringing field at the patch periphery and then the radiated power. Thus the use of high permittivity superstrate ε_{r2} leading to high ratio $\varepsilon_{r2}/\varepsilon_{r1}$ is possible and

(a)

(b)
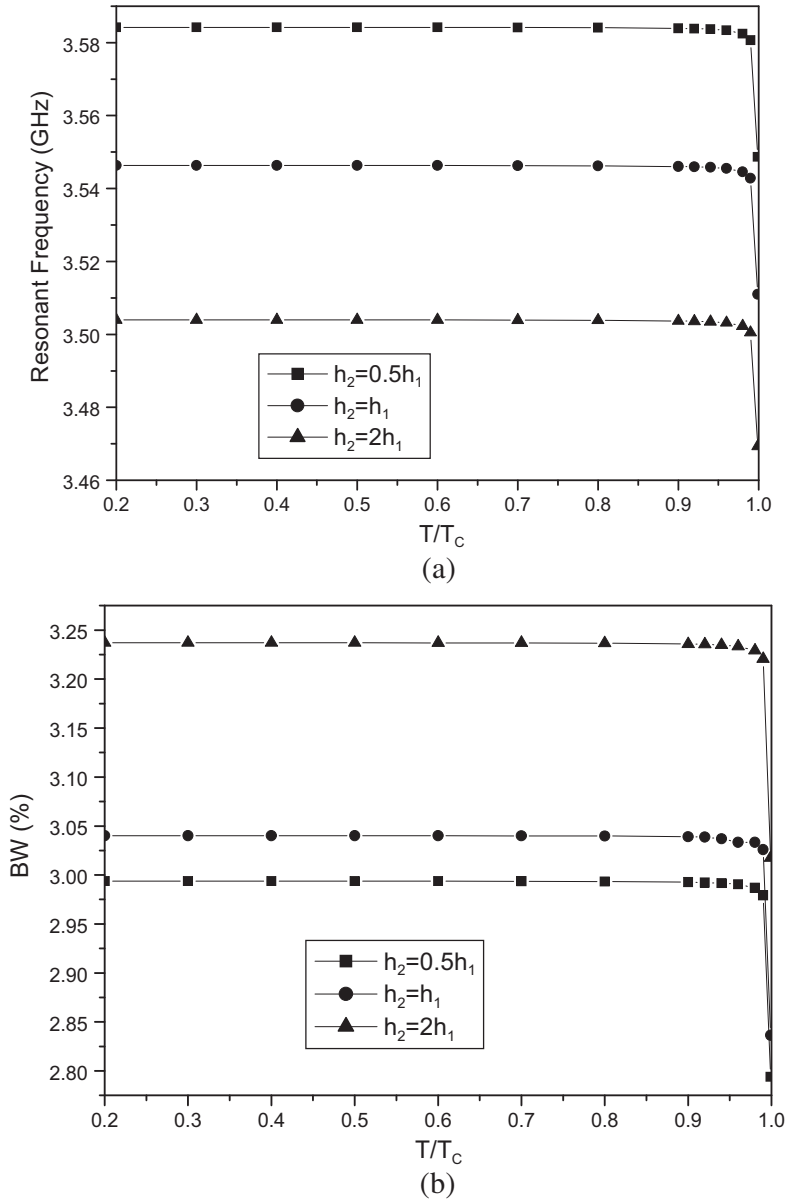
Figure 5. Resonance frequency and half-power bandwidth of the high T_c superconducting printed patch with different thicknesses of superstrate layer against operating temperature; $\sigma_n = 210.10^3$ S/m, $\lambda_0 = 150$ nm, $a = 15$ mm, $\varepsilon_{1x} = \varepsilon_{1z} = \varepsilon_{2x} = \varepsilon_{2z} = 2.32$, $h_1 = 1.5748$ mm, $e = 0.02$ µm. (a) Resonance frequency. (b) Half-power bandwidth.

Table 1. Comparison of measured and calculated resonant frequencies for isotropic substrate-superstrate configuration. $h_1 = 1.57\,\text{mm}$, $\varepsilon_{1X} = \varepsilon_{1Z} = 2.05$, and $\text{tg}(\delta) = 0.00045$.

h_2 (mm)	f_r (GHz) (MoM. Chebyshev polynomials)	f_r (GHz) Our measurements results	Errors (%)
0	1.136	1.128	0.71
1.5748	1.126	1.104	1.99
3.1496	1.122	1.100	2.00

could give significant improvements under condition of sufficient thickness indeed. From Figure 3(b), we can note that for ratios h_2/h_1 less than 1.5, the bandwidth is degraded, especially as the permittivity ε_{r2} of the superstrate is high.

In the two studies that follow, the permittivity of superstrate is chosen such as $\varepsilon_{r2}/\varepsilon_{r1} = 1$, and the results are given for 3 ratios h_2/h_1. Other parameters remain unchanged from those of Figure 4.

The influence of superconducting film thickness is reported in Figure 4.

As the thickness grows, resonant frequency and half-power bandwidth of the printed disc increase quickly until the thickness reaches the penetration depth λ_0. After this value, increasing the superconducting thickness does not produce any significant change for the resonant frequency and half-power bandwidth.

Finally, the effects of the operating temperature are investigated in Figure 5. A negligible influence on the resonant characteristics of the HTS printed antenna is observed except for values near the critical temperature T_c. For temperatures around T_c, a fast decrease of resonant frequency and half-power bandwidth occurs.

5. CONCLUSION

In millimeter waves applications, when dimensions of printed antennas become very small, high losses occur leading to poor efficiency. In order to reduce them, the use of HTS material for the radiating patch has been introduced [5–9]. In addition to an increased radiated power, low losses mean low noise, small dispersion and smaller devices. These improved features lead to greater integration density and reduced signal propagation time. Thus HTS printed antennas are well suited for today's fast communications.

This paper describes a full-wave spectral analysis of the resonant characteristics of HTS circular patch. The rigorous approach is based on a Galerkin's moment method, and the complex resonance frequencies are studied with combinations of Chebyshev polynomials with weighting factors in conjunction with the complex resistive boundary condition [14, 18]. Calculated resonant frequencies are compared with experimental results from literature, and excellent agreements are found. Comparison with recent published results using different methods [15] and different types of expansion basis functions of the disk current (the TM and TE modes of cavity) [20] is also proposed.

The influence of a dielectric protective cover is investigated showing interesting enhancement on the resonant characteristics of HTS circular printed antenna. In addition to a decrease of the resonant frequency, a thick superstrate with high permittivity leads to significant increase of the half-power bandwidth. Considering the current need for integration and the ever-increasing signal bandwidth, these effects may be of interest in the design of superconducting printed antennas.

REFERENCES

1. Kumar, G., *Broadband Microstrip Antennas*, Artech House, Boston London, 2003, ISBN 1-58053-244-6.
2. Pozar, D. M., "Considerations for millimeter wave printed antennas," *IEEE Transactions on Antennas and Propagation*, Vol. 31, 740–747, 1983.

3. Viani, F., L. Lizzi, M. Donelli, D. Pregnolato, G. Oliveri, and A. Massa, "Exploitation of parasitic smart antennas in wireless sensor networks," *Journal of Electromagnetic Waves and Applications*, Vol. 24, No. 7, 993–1003, 2010.

4. Febvre, P. and M. Donelli, "An inexpensive reconfigurable planar array for Wi-Fi applications," *Progress In Electromagnetics Research C*, Vol. 28, 71–81, 2012.

5. Nisenoff, M. and J. Pond, "Superconductors and microwaves," *IEEE Microwave Magazine*, Vol. 10, No. 3, 84–95, 2009.

6. Hansen, R. C., *Electrically Small, Superdirective, and Superconducting Antennas*, John Wiley& Sons, Inc, Hoboken, New Jersey, 2006.

7. Fortaki, T., M. Amir, S. Benkouda, and A. Benghalia, "Study of high Tc superconducting microstrip antenna," *PIERS Online*, Vol. 5, No. 4, 346–349, 2010.

8. Khamas, S. K., M. J. Mehler, T. S. M. Maclean, and C. E. Gough, "High-T/sub c/superconducting short dipole antenna," *Electronics Letters*, Vol. 24, No. 8, 460–461, 1988.

9. El-Ghazaly, S. M., R. B. Hammond, and T. Itoh, "Analysis of superconducting microwave structures: Application to microstrip lines," *IEEE Trans. Microwave Theory Tech.*, Vol. 40, No. 3, 499–508, 1992.

10. Benkouda, S., A. Messai, M. Amir, S. Bedra, and T. Fortaki, "Characteristics of a high Tc superconducting rectangular microstrip patch on uniaxially anisotropic substrate," *Physica C: Superconductivity*, Vol. 502, 70–75, July 2014.

11. Bedra, S. and T. Fortaki, "Effects of superstrate layer on the resonant characteristics of superconducting rectangular microstrip patch antenna," *Progress In Electromagnetics Research C*, Vol. 62, 157–165, 2016.

12. Bedra, S. and T. Fortaki, "High-Tc superconducting rectangular microstrip patch covered with a dielectric layer," *Physica C: Superconductivity and Its Applications*, Vol. 524, 31–36, May 2016.

13. Barkat, O., "Theoretical study of superconducting annular ring microstrip antenna with several dielectric layers," *Progress In Electromagnetics Research*, Vol. 127, 31–48, 2012.

14. Benmeddour, F., C. Dumond, F. Benabdelaziz, and F. Bouttout, "Improving the performances of a high Tc superconducting circular microstrip antenna with multilayered configuration and anisotropic dielectrics," *Progress In Electromagnetics Research C*, Vol. 18, 169–183, 2011.

15. Bedra, S., R. Bedra, S. Benkouda, and T. Fortaki, "Efficient CAD model for the analysis of high Tc superconducting circular microstrip antenna on anisotropic substrates," *Advanced Electromagnetics*, Vol. 6, No. 2, May 2017.

16. Losada, V., R. R. Boix, and M. Horno, "Resonant modes of circular microstrip patches in multilayered substrates," *IEEE Trans. Microwave Theory Tech.*, Vol. 47, No. 4, 488–498, 1999.

17. Tulintsef, A. N., S. M. Ali, and J. A. Kong, "Input impedance of a probe-fed stacked circular microstrip antenna," *IEEE Transactions on Antennas and Propagation*, Vol. 39, 381–390, Mar. 1991.

18. Garg, R., P. Bhartia, I. J. Bahl, and A. Ittipiboon, *Microstrip Antenna Design Handbook*, Artech House, Inc, 2001.

19. Fang, D. G., *Antenna Theory and Microstrip Antennas*, Taylor and Francis Group, 2010.

20. Bedra, S., R. Bedra, S. Benkouda, and T. Fortaki, "Superstrate loading effects on the resonant characteristics of high Tc superconducting circular patch printed on anisotropic materials," *Physica C: Superconductivity and Its Applications*, Vol. 543, 1–7, December 2017.

21. Richard, M. A., K. B. Bhasin, and P. C. Claspy, "Superconducting microstrip antennas: An experimental comparison of two feeding methods," *IEEE Transactions on Antennas and Propagation*, Vol. 41, 967–974, 1993.